A HIGH-RESOLUTION UNDERWATER ACOUSTIC COMMUNICATION PROPAGATION SIMULATOR WITH MULTI-PATH TRANSIENT SEA-SURFACE INTERACTIONS

Michael Caley[1] and Alec Duncan[1]

[1]Centre for Marine Science and Technology
Curtin University, Perth WA 6845, Australia
Email: michael.caley@student.curtin.edu.au

Abstract

A channel simulation has been developed to explore the fine time-scale Doppler and multi-path arrival-time delay spreading imparted to underwater communication signals by interaction with the transient ocean surface. The simulation provides a configurable ocean test-bed for the purpose of testing and developing acoustic signal data coding and decoding strategies that are more reliable and resistant to the natural reverberation, arrival delay distortion and Doppler distortion that are inherent in relatively shallow underwater signal propagation. The simulator operates by calculating the transmit impulse response for successive realisations of a three-dimensional ocean surface with configurable sea and swell parameters. A unique transmit impulse response history is calculated for each of the underlying flat-surface ray-paths, capturing time-varying fluctuations of the rough surface around the mean-plane response. The realism of the synthetic multi-path channel response history is then evaluated against an experimental channel.

1. Introduction

The transmission of data underwater in a stream of acoustically coded characters is subject to all of the adverse reverberation effects we are familiar with in the context of speech intelligibility in an auditorium, but with a few complications. Think of the ocean, with the swell and sea surface shape frozen in time, and you have an underwater 'auditorium' or perhaps closer to a stone cathedral, with an elaborately profiled 99% acoustically reflective 'ceiling'. After a little while you adapt to the multi-path reflections in this 'frozen surface' auditorium, and can follow the speaker.

But then the 'ceiling' becomes completely alive, oscillating in waves of all sizes, so that the room reverberation is constantly wavering, the speakers voice has become possessed by a strange Doppler vibrato, whilst the ceiling may create some of its own sound as it tumbles and hisses. A nearby school of fish are chatting, and snapping shrimp sitting beside you are 'popping gum' almost in your ear. Half-way through the speakers address, the sound-speed profile becomes vertically stratified, so the direct sound-path vanishes. Situation normal for underwater acoustic communication.

In the marine environment some strategies for coding/decoding data acoustically are better than others. A strategy that works well at one range and surface condition must be adapted for other conditions. The focus of this work is the development of a simulation that enables an arbitrary acoustically transmitted data signal to be realistically distorted in the manner of the infinitely variable real ocean.

2. Simulation Overview

An underwater acoustic communication channel simulator has been developed to model transmission of a continuous spectrum communication signal $x(t)$ within the nominal bandwidth of 8 kHz to 16 kHz sampled at 96 kS/s, to generate an output pressure signal $y(t)$ at 96 kS/s. The simulation is valid at relatively high frequencies at which sound propagation through the water and reflections off the sea-bed may be approximated using ray-acoustics. The simulation is typically used to create a 30 second duration time-circular channel response $h(t, \tau)$ that can be convolved with a transmit signal of any length as shown in Fig.1. The nominal 30 second duration for the circular channel response is chosen to capture transient effects of ocean swell, with typical wave periods of 15 seconds and less.

The model implementation relates to a constant depth and constant-with-range sound-speed gradient environment. The sub-millisecond scale transient delay and Doppler distortion of a continuous transmit signal is calculated in response to a time-series of 3D Gaussian surface realisations, derived from a directional surface-wave spectrum for each of swell and wind-driven waves.

Earlier channel-probing experiments supporting the simulation model development were conducted near Cottesloe in 13.5 m water depth [1], and near Rottnest Island in 53 m water depth near Perth, Western Australia, over ranges from 100m to 10km, utilising the point-source point-receiver arrangement shown schematically on Fig. 2. All trials were conducted with the receiver within 1.5 km of a Directional Wave-Rider Buoy that records and updates the directional surface-wave spectrum at 15 minute intervals.

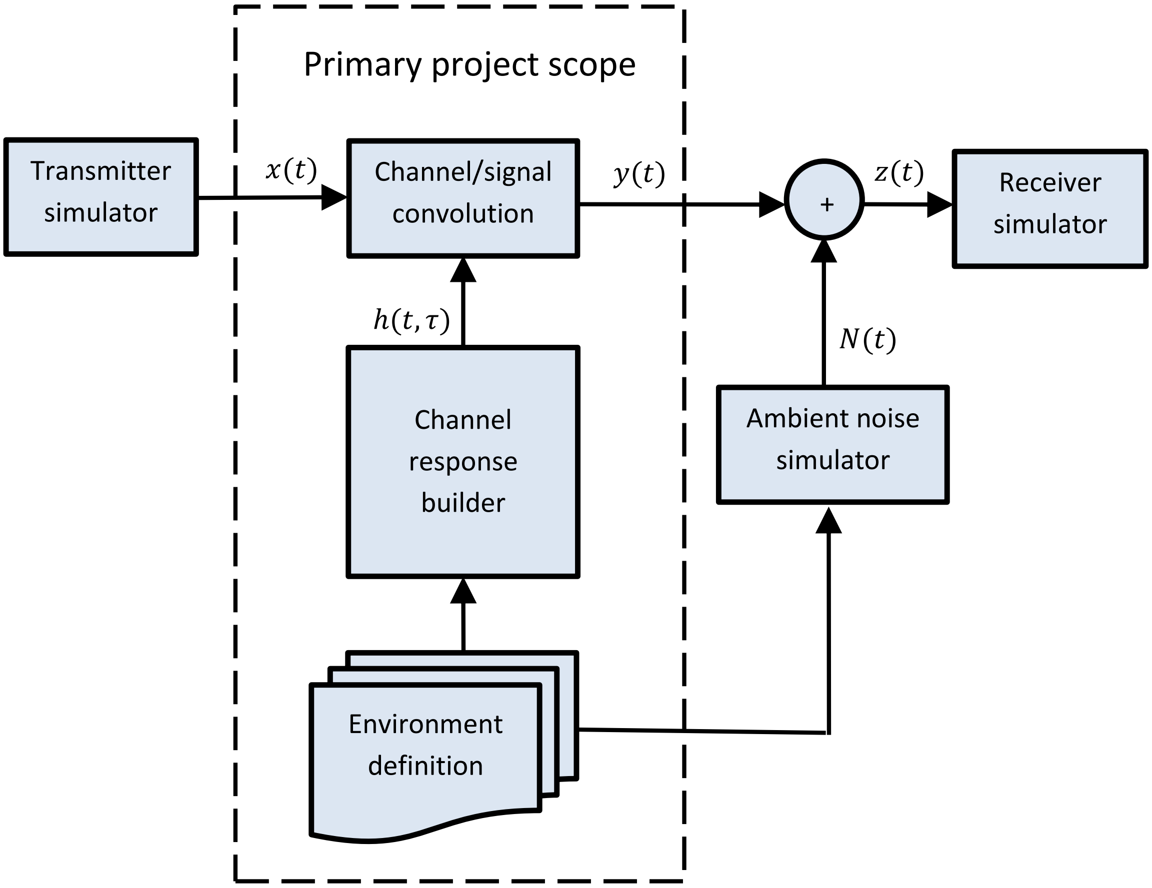

Figure 1. Simulation structure

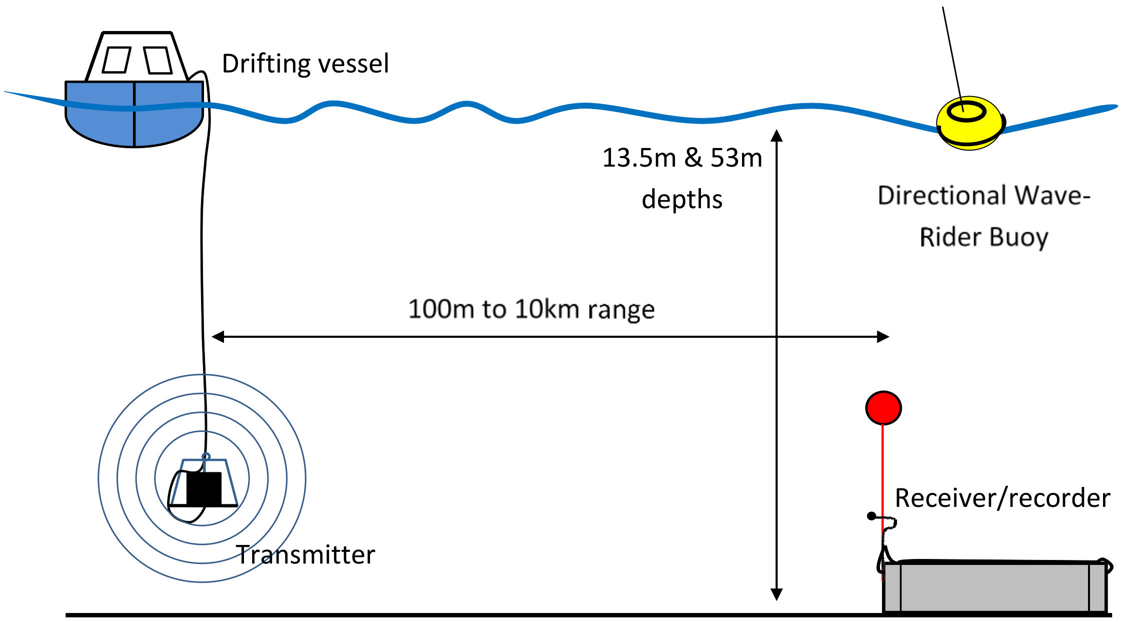

Figure 2. Schematic channel probe arrangement

3. Example Underwater Acoustic Data Communication Signal

The spectral appearance of a series of spread-spectrum communication signals is illustrated on Fig.3, to emphasise that the simulator needs to be capable of transmitting signals with a continuous frequency spectrum. Spread-spectrum signalling is a widely used strategy that enables fast data transmission rates and resistance to transient frequency-selective fading within the channel bandwidth. Spread-spectrum signalling from the source is derived from a set of pseudo-random binary (i.e. {0,1}) sequences, or symbols. In the Fig.3 example, which represents the transmission of around 7000 such symbols, each successive symbol was created using successive binary sequences to phase-switch a 12 kHz sinusoidal carrier tone at the binary 'chipping' rate of 3 kHz. The 'impulsive' or abrupt phase-switching causes the spreading of the binary information across the transmission bandwidth. The frequency spreading of the transmit signal is continuous in the frequency domain. The simulator must therefore be able to 'seamlessly' transform signals of any frequency composition within the design channel bandwidth. At the receiver end, spread-spectrum acoustic signalling relies on the identification of phase-shifts in the received signal. Accordingly, the simulator should not introduce extraneous abrupt phase-shifts.

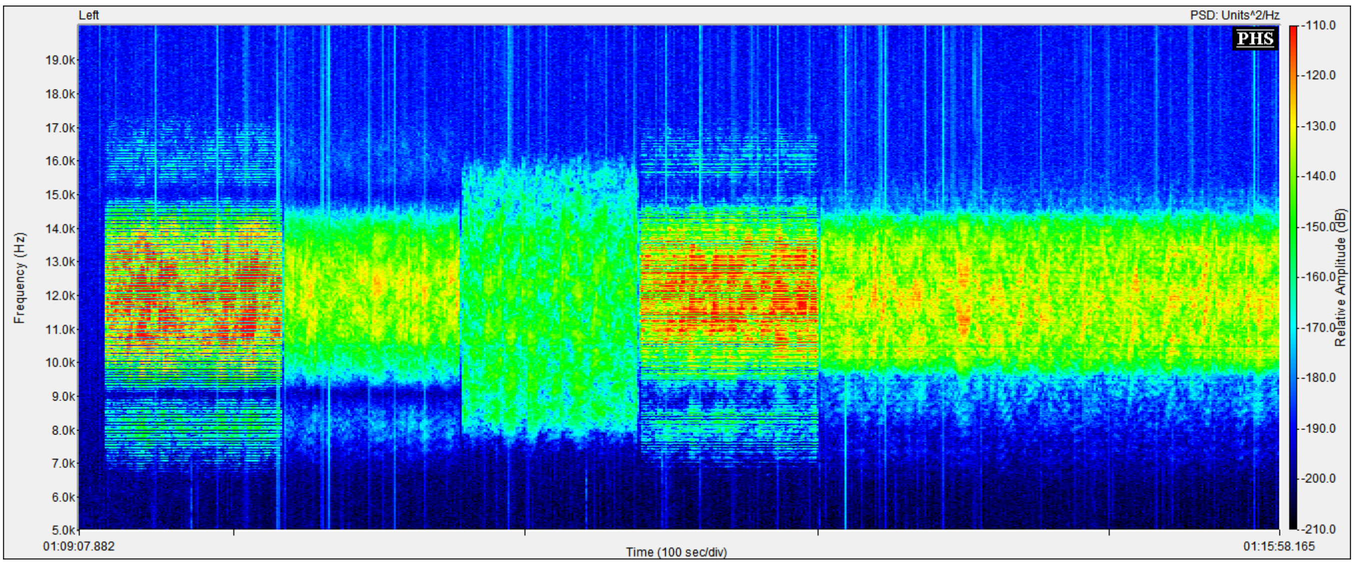

Figure 3. Experimental spectrogram for 6 minutes of received spread-spectrum signal at 2km range

4. Simulation of the Ideal Flat-Surface Ocean Channel

For the flat-surface condition, the received signal can be understood as the sum of overlapping delayed, amplitude-scaled and phase-shifted replicas of the original transmit signal $x(t)$ along ray Eigen-paths as shown schematically on Fig. 4, and calculated by Eq. (1).

Figure 4 shows the first 6 arrivals out of a theoretically infinite number of 'reverberant' arrivals with increasing numbers of surface interactions. Each path has a received complex amplitude scale factor A_n that includes the path phase shift, and path delay τ_n. The delay accords to the transmission path-length, and the amplitude is scaled by geometrical spreading, sea-water attenuation and the calculated bottom reflection loss. These ray-path transmission parameters have been calculated using the Bellhop [2] ray propagation model.

$$y(t) = \sum_{n=1}^{N} A_n x(t - \tau_n) \tag{1}$$

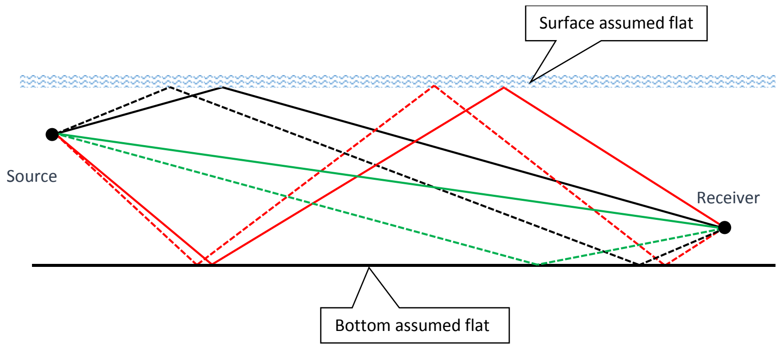

Figure 4. First six Eigen-path ray arrivals for simple iso-speed channel

5. Rough Ocean Surface Calculation Methodology

5.1 Simulation calculation structure

The simulation structure combines the time-invariant flat-surface ray-path response calculated by the ray-tracing model, with a time-varying transient response to the rough surface, implemented by a set of Finite Impulse Response (FIR) filter cascades.

For the n^{th} ray-path, the FIR representing the channel response for a 'snapshot' of the rough surface profile is calculated initially in the frequency domain, as the product of the average flat-surface ray-path pressure amplitude response, $A_{n,flat}$, and an 8-16 kHz Fourier-synthesised approximation, $H_{n,rough}(\omega)$, to the rough-surface pressure response, (or frequency transfer function) relative to the flat-surface response as per Eq. (2).

$$H_{n,path,}(\omega) = A_{n,flat} H_{n,rough}(\omega) \tag{2}$$

For a multiple surface-bounce path, the rough-surface frequency-domain pressure response is approximated as the product of n_{top} bi-static rough patch responses as per Eq. (3).

$$H_{n,rough}(\omega) = \prod_{j=1}^{n_{top}} H_{n,patch,j}(\omega) \tag{3}$$

A new estimate of $H_{n,rough}(\boldsymbol{t}, \omega)$ is calculated periodically for a time-series of 3D rough-surface realisations, nominally at 20ms intervals. The total signal output $y(t)$ is then calculated as the sum of the inverse-transformed transient path responses $h_{n,path,}(\boldsymbol{t}, \tau)$ convolved with the corresponding copy of the input signal $x_n(t)$ as per Rq. (4). The real time symbol within the FIR response is shown as $\boldsymbol{t}$, to indicate that the response $h_{n,path,}(\boldsymbol{t},\tau,)$ is utilised circularly with respect to t. The input signal copy $x_n(t)$ for the n^{th} base path is Doppler shifted to incorporate relative transmitter/receiver platform movement resolved into the base-path launch direction.

$$y(t_j) = \sum_{n=1}^{N \text{ base paths}} \left\{ \sum_{m=1}^{M \text{ FIR delays}} h_{n,path}(\boldsymbol{t}_{(i+m-1)}, \tau_{(M-m+1)}) \;\; x_n(t_{(i+m-1)} - \bar{\tau}_n) \right\} \tag{4}$$

On each path the response is updated at the signal sampling rate, so each input signal sample $x(t_i)$ is convolved with a unique interpolated path response $h_{n,path,}(\boldsymbol{t},\tau)$. At any instant in time, the single path output value is the summation of M sequential micro-path FIR outputs, each representing a 'static' channel response. The flat-surface ray-path delay is shown with a bar $\bar{\tau}_n$, to distinguish it from the variable delay τ_m within the calculated rough surface response FIR.

5.2 Rough surface-bounce response calculation

The frequency domain rough-surface pressure response $H_{patch}(\omega)$ for a single surface interaction with a 'snapshot' of the real moving surface (such as Fig. 5), may be approximated by discretising a limited patch of a 3D synthesised rough surface. The scattered field from the surface may be approximately computed by making the Kirchhoff Approximation on the scattering surface, that the scattered pressure at the surface is equal and opposite to the incident pressure [3].

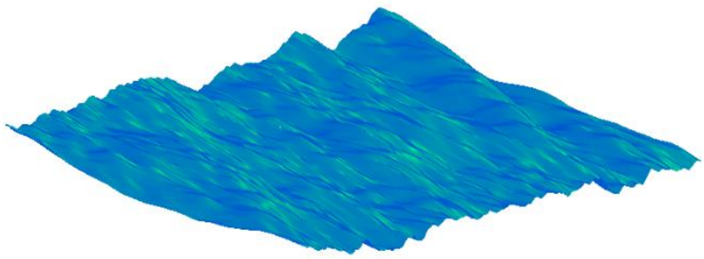

Figure 5. Synthesised surface realisation utilising WAFO Toolbox [4]

The Kirchhoff approximate response of each surface element may be calculated by (5), based on the geometry in Fig. 6, where k_0 denotes the incident acoustic wavenumber, and the prime ($'$) denotes quantities in the local coordinate system of the element. The element dimensions in local $x'$and y' directions are $a'$and b'. After converting the response from the local facet coordinates to the global x, y, z coordinates, the individual element pressure contributions are then coherently summed over the rough-surface patch for each frequency within the bandwidth of interest, to obtain the frequency-domain rough patch pressure response $H_{patch}(\omega)$ by Eq. (6).

The expression $(R_0 + R_r)(-1)\, e^{-ik(R_0 + R_r)}$ in (6) normalises the response by the flat-surface specular path range, and removes the phase-change associated with the surface reflection and path-range, so that the result can be combined with the flat-surface ray-path response $A_{n,flat}$ without duplicating geometric spreading and phase changes already included in the flat-surface ray-path model. The mean-plane specular radii R_0 and R_r are identified on Fig. 7.

$$p_r(\omega) = \frac{i}{2\pi} \sum_{i,j} \frac{k'_{0z} e^{ik(r_0+r_r)}}{r_0 r_r} a' \operatorname{sinc}\left[\frac{a'}{2\pi}(k'_{rx} - k'_{0x})\right] b' \operatorname{sinc}\left[\frac{b'}{2\pi}(k'_{ry} - k'_{0y})\right] \tag{5}$$

$$H_{patch}(\omega) = \textstyle\sum_{\text{patch}} p_r(\omega)\,(R_0 + R_r)(-1)\, e^{-ik(R_0 + R_r)} \tag{6}$$

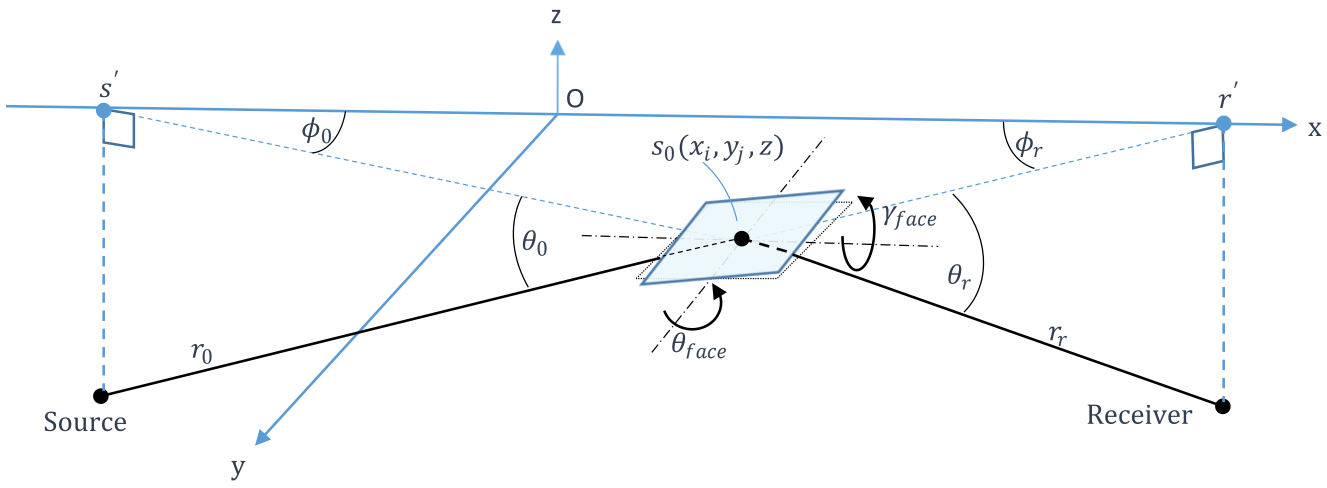

Figure 6. Geometry for response from surface element

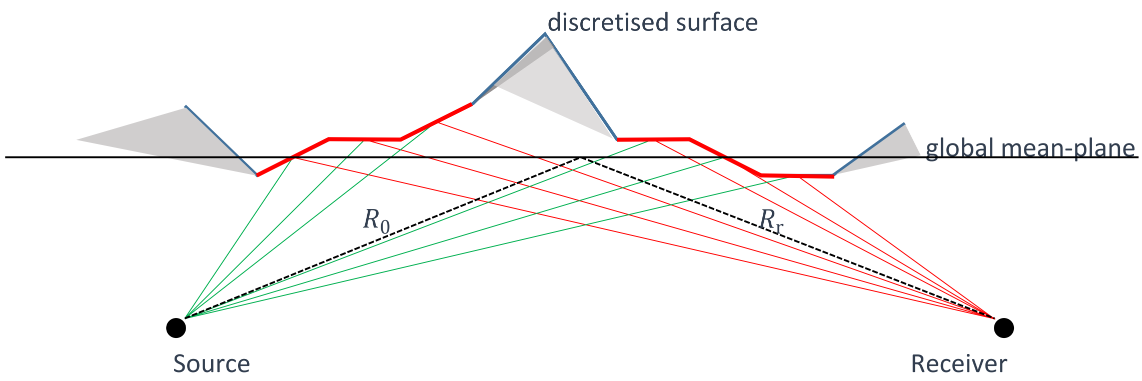

Figure 7. Geometry for summation of bi-statically illuminated facet contributions

6. Simulation Results

6.1 Channel response for nearly flat surface

Figure 8 illustrates the simulated near-flat-surface channel response history for 120m range, with the transmitter 3.5m off the bottom and the receiver 1m off the bottom in a 13.5m deep channel. In this example the swell was set to 1cm significant wave height, with 13.5s period, together with 1cm significant wind-wave height, with 3s period. Each line of this response history represents a persistent (in time) replica of the transmit signal. The response is calculated at 96kS/s in the delay dimension, and at 20ms intervals in the real-time (vertical) dimension.

For this simplified channel response, the entire data communication could be extracted at the receiver by 'tuning-in' the receive-signal correlator to the delay corresponding to any (or all) of the ray-paths, as a complete and continuous signal replica is transmitted via each ray-path. The bottom-bounce path is very closely spaced to the direct path near 0 ms delay, due to both the source and receiver being close to the bottom.

6.2 Channel response with low swell only

The simulation is now modified by the introduction of a realistic swell spectrum similar to the low wave conditions experienced experimentally for the 2012 Cottesloe trial. This spectrum is characterised by a significant wave height of 0.4 m, and a peak period of 13.5 s. Spectral components up to 1/6 Hz were included. The higher frequency wind-waves have been excluded from the simulation for this example.

With the introduction of low swell, the time-varying delay of surface-interacting paths is observed on Fig. 9. The four single-surface bounce path permutations are observed centred on approximately 2 ms delay, with the four double-surface bounce path permutations on the right-hand side of Fig. 9. From a communication perspective the full data communication could still be extracted from any or all of the path arrivals.

6.3 Channel response with complete surface consisting of low swell and wind waves

The high-frequency wind wave spectrum is now added to the definition of the surface simulation. This spectrum is characterised by a significant wave height of 0.25 m and peak period of 1.9 s which correspond to conditions recorded during the Cottesloe experiment. Spectral components up to 1 Hz were included.

The higher-frequency surface waves have a marked effect on the delay-spreading of the surface-reflected paths, such that the continuous extraction of the signal data is now only straightforward for the non-surface interacting (i.e. direct and bottom-bounce) paths.

It is not uncommon in the underwater environment for sound refraction to prevent direct-path propagation between a source and receiver, and in some instances there is no bottom-bounce path either. In these circumstances communication must partly or fully rely on signal that has arrived via one or more interactions with the sea-surface, illustrated by the intermittent and arrival delay-spread responses on Fig. 10.

6.3 Frequency spreading of the received signal for surface with low swell and sea waves

Up to this point there has been no mention of the frequency shifts that are created in the received signal by the constantly changing rough-surface propagation paths.

A useful tool for simultaneously examining the arrival delay spreading and the Doppler spreading of the received signal is the ‘spreading function’, as described in [5]. A spreading function over the delay-Doppler plane is obtained by discrete Fourier transform of a history $h(t,\tau)$with respect to the real-time (t) dimension as per Eq. (7). The Doppler shift units of Hz are relative to the simulation bandwidth centre frequency of 12 kHz.

$$S(\nu,\tau) = \mathcal{F}(h) = \sum_{n=1}^{N-1} h(t_n,\tau)\exp(-i2\pi n\nu) \tag{7}$$

In Fig. 11 the spreading functions for the previously described swell-only simulation (left) and the swell-plus-sea simulation (right) are presented. It may be seen that the addition of higher-frequency surface waves not only greatly spreads the arrival time via ‘micro-paths’ but the Doppler shifts are also substantially increased and dispersed. No frequency spreading is observed for the direct and bottom-reflected paths that are almost coincident at zero delay (relative to direct path).

In the design of digital signal processing decoding strategies for an underwater acoustic communication receiver, the potential Doppler deviations in the received signal need to be known to optimise the receiver recognition of the incoming character stream. The ability to realistically simulate this Doppler and delay spread for different transmitter-receiver geometries benefits this design process.

7. Example comparison between a measured and simulated channel response

Fig. 12 illustrates an example comparison of the experimentally measured channel response (left images) and the synthetically generated channel response (right images), complete with the effect of vessel drift and vertical motion of the transmitter. Notwithstanding the inherent recording limitations in the match between the experimental and simulated surface, the comparison illustrates that the model is able to realistically simulate the scale of frequency and arrival delay spreading. Similar favourable comparisons have been made at ranges up to 1 km at 13.5 m depth, and at ranges from 100 m to 8 km at 53 m depth.

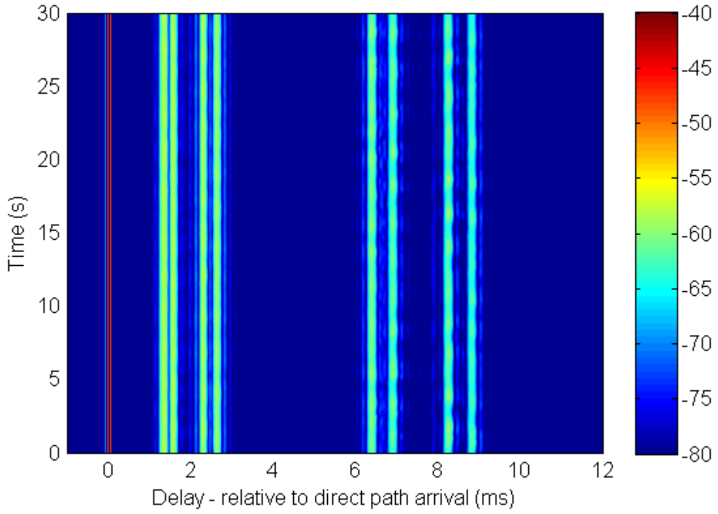

Figure 8. Flat surface channel response history, $10.\log_{10}|h(t,\tau)|^2$ including first ten ray-paths

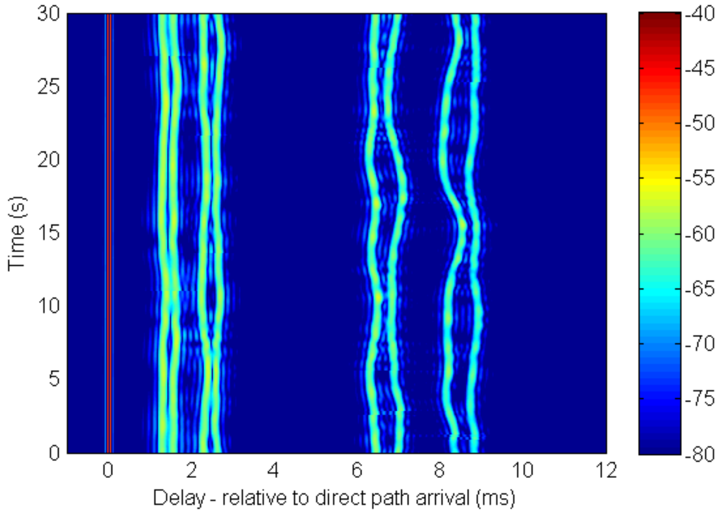

Figure 9. Low-frequency swell-only channel response history, $10.\log_{10}|h(t,\tau)|^2$

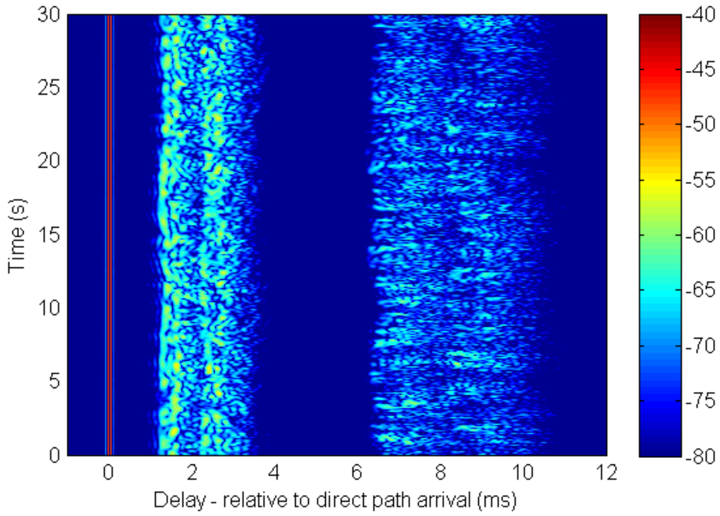

Figure 10. Low amplitude swell and sea channel response history, $10.\log_{10}|h(t,\tau)|^2$

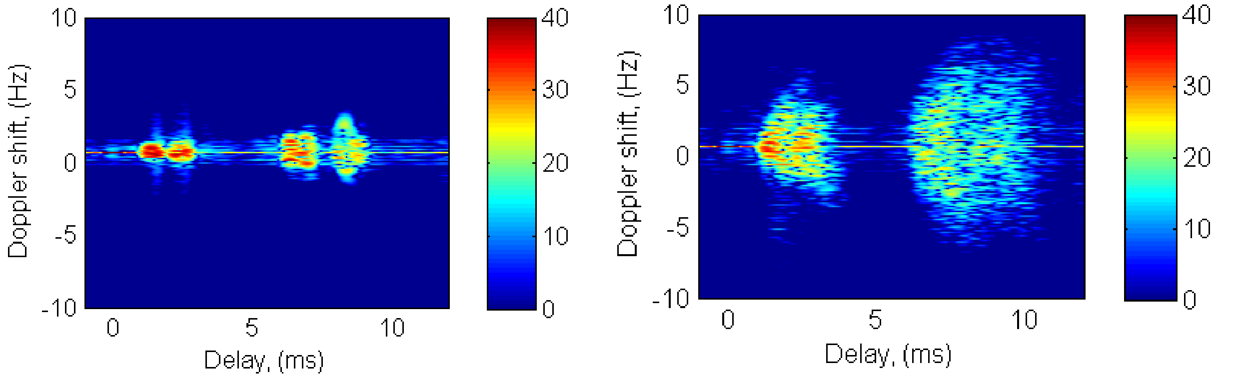

Figure 11. Spreading function, $10.\log_{10}|S(\nu,\tau)|^2$ for swell only (left), and swell plus sea (right)

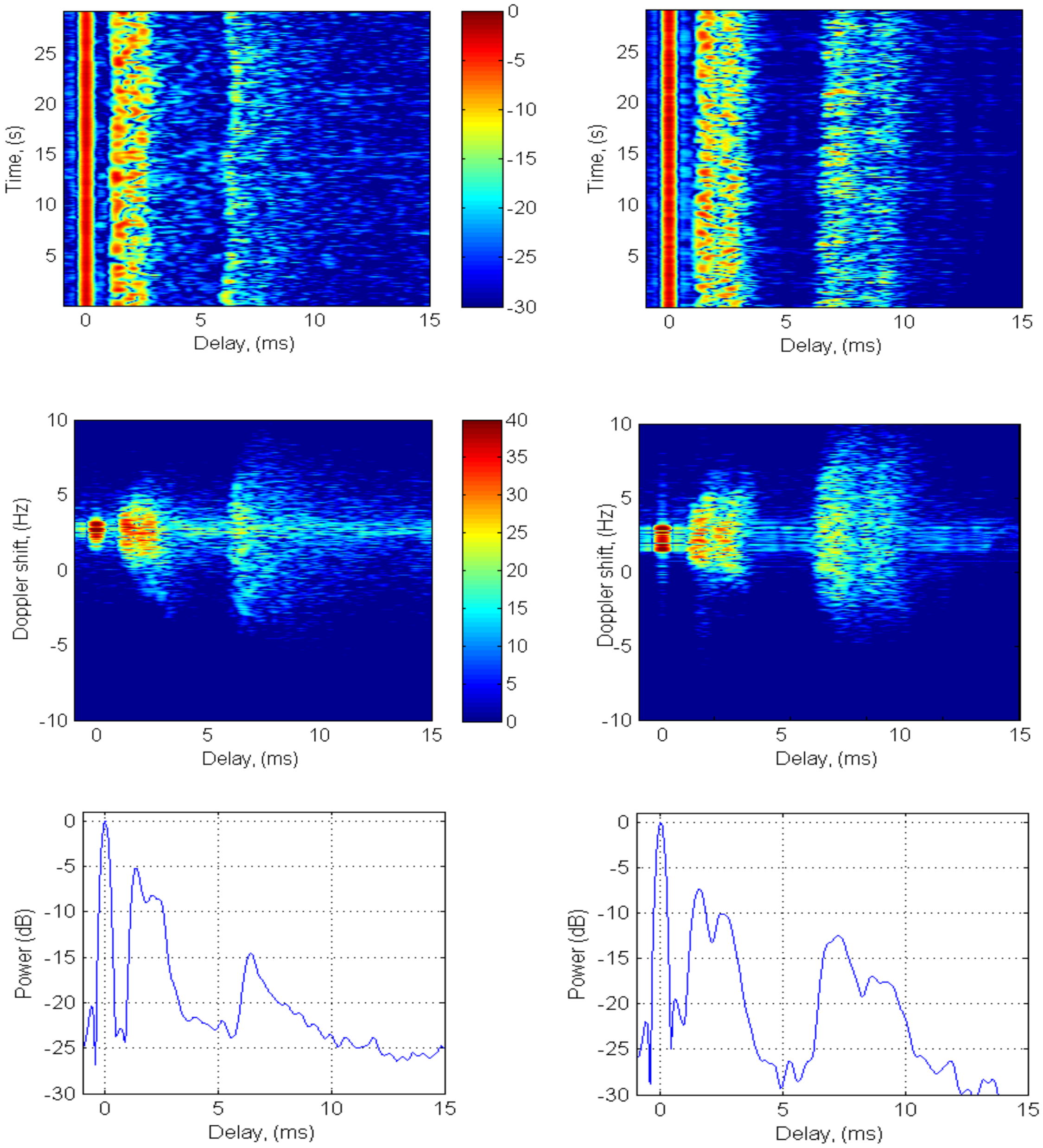

Figure 12. Experimental channel characteristics (left), and synthetic channel characteristics (right), for (top) channel response history $10.\log_{10}|h(t,\tau)|^2$, (middle) spreading function $10.\log_{10}|S(\nu,\tau)|^2$, and (bottom) arrival delay power response $10.\log_{10}P(\tau)$

8. Summary

An underwater acoustic channel simulation method has been developed based on an approximate quantitative model of the rough surface response. It has been demonstrated by simulated transmission of a spread-spectrum probe signal identical to that used experimentally, then comparison of the signal delay and Doppler spreading of the synthetic and experimental channels, that the model is capable of reproducing fine-time-scale Doppler and delay distortions typical of those generated in real shallow water ocean channels.

The model provides a powerful tool by which the received signal delay and Doppler spreading for specific surface-wave conditions and channel geometries may be directly explored. This is beneficial in the context of the design of underwater communication coding and decoding strategies, and hardware development. It is also beneficial in selection of deployment positioning for underwater communication systems.

There is considerable scope to extend the modelling methodology to simulate situations with more challenging relative movements of the transmitter and receiver. Another worthwhile area for further development is the hardware implementation of the simulator, so that simulations can directly interface with underwater modems. For this to occur the simulation algorithms need to be implemented at machine-code level in a parallel processing architecture to enable real-time simulation.

Acknowledgements

This project is supported under the Australian Research Council's Discovery Projects funding scheme (project number DP110100736) and by L3-Communications Oceania Ltd.

References

[1] Caley, M. and Duncan, A. "Investigation of underwater acoustic multi-path Doppler and delay spreading in a shallow marine environment", *Acoustics Australia*, **41**(1), 20-28, (2013).

[2] Porter, M.B. The BELLHOP Manual and Users Guide, 2011. http://oalib.hlsresearch.com/Rays/HLS-2010-1.pdf

[3] Ogilvy, J.A. *Theory of Wave Scattering from Random Rough Surfaces*, Bristol, Great Britain: Adam Hilger, pp.73-112, 1991.

[4] WAFO Group, *WAFO - A Matlab Toolbox for Analysis of Random Waves and Loads - A Tutorial*, Math. Stat., Center for Math. Sci., Lund Univ., Lund, Sweden. URL http://www.maths.lth.se/matstat/wafo, 2000.

[5] van Walree, P. A. Channel sounding for acoustic communications: techniques and shallow-water examples, FFI report 2011/00007: Norwegian Defence Research Establishment, 2011. http://www.ffi.no/no/rapporter/11-00007.pdf